Applied Surface Science 413 (2017) 381–386

Contents lists available at ScienceDirect

Applied Surface Science

journal homepage: www.elsevier.com/locate/apsusc

Full Length Article

Hierarchical structure graphitic-like/MoS_2 film as superlubricity material

Zhenbin Gong [a,b], Xiaolong Jia [c], Wei Ma [a], Bin Zhang [a], Junyan Zhang [a,*]

[a] State Key Laboratory of Solid Lubrication, Lanzhou Institute of Chemical Physics, Chinese Academy of Sciences, Lanzhou 730000, China
[b] University of Chinese Academy of Sciences, Beijing, 10049, China
[c] School of Material Science and Engineering, Lanzhou University of Technology, Lanzhou 730050, China

ARTICLE INFO

Article history:
Received 9 January 2017
Received in revised form 7 April 2017
Accepted 7 April 2017
Available online 8 April 2017

Keywords:
Hierarchical structure
Graphitic-like/MoS_2
Thin film
Engineering
Superlubricity

ABSTRACT

Friction and wear result in a great amount of energy loss and the invalidation of mechanical parts, thus it is necessary to minimize friction in practical application. In this study, the graphitic-like/MoS_2 films with hierarchical structure were synthesized by the combination of pulse current plasma chemical-vapor deposition and medium frequency unbalanced magnetron sputtering in preheated environment. This hierarchical structure composite with multilayer nano sheets endows the films excellent tribological performance, which easily achieves macro superlubricity (friction coefficient ~0.004) under humid air. Furthermore, it is expected that hierarchical structure of graphitic-like/MoS_2 films could match the requirements of large scale, high bear-capacity and wear-resistance of actual working conditions, which could be widely used in the industrial production as a promising superlubricity material.

1. Introduction

Generally, there is friction and wear existing between moving parts in mechanical system. These friction and wear will result in a great amount of energy loss and failure of mechanical parts, which, in turn, will affect the efficiency and lifespan of mechanical equipments. According to statistics, the loss resulted from friction and wear takes up a growing proportion of the Gross National Product each year in industrialized countries [1]. Therefore, it appears quite essential to reduce the friction and wear between mechanical parts.

Superlubricity, proposed firstly by Hirano and Shinjo in 1990s, is a significant mean to essentially deal with the friction and wear mentioned above, which refers that the friction between two surfaces is close to zero [2]. In theory, the superlubricity can arrive at near-zero friction and wear, whereas the friction coefficient at the degree of 0.01 or lower is regarded as superlubricity [3], due to the interference of various factors and the limitation of measurement. Typically, two types of materials have been found the features of the superlubricity: one is the solid lubricants deposited on the surface, such as MoS_2, graphite, diamond-like carbon films (DLC) and carbon nitrogen film (CNx) [4–7], the other is molecularly thin layers confined in contact surfaces, such as water lubrication of ceramic [8], polymer brush [9,10] and hydration lubrication [11,12]. However, most superlubricity systems are difficult to be applied in engineering, since the surface property diminished soon at macro scale or under high normal load.

Recently, molybdenum disulfide (MoS_2) has attracted great attention [13,14], due to its special hexagonal layered structure. This unique two-dimensional structure, owing to the weak shear strength between the layers, endows the corresponding composites with well tribological performance. Martin et al. [15] obtained ultra low friction coefficient less than 0.002 for MoS_2 films under high vacuum and discovered that the MoS_2 crystal overlapping and rotating a certain angle in the friction process by observing the wear debris through transmission electron microscopy. So, the incommensurate contact between the MoS_2 crystals can be the true reason for super lubrication. In addition, Chhowalla et al. [16] have successfully developed the thin films composed by fullerene-like MoS_2 spherical particles, whose friction coefficient can reach at 0.003 in humid air [16]. The reason for the superlubricity of fullerene-like MoS_2 thin film is that curved S-Mo-S structure effectively hindered the surface from oxidizing and protected the layered structure.

Graphite and MoS_2 have quite similar layer structure with complementary physical properties [17]. In a certain situation, the crystal graphite can realize superlubricity, owing to the incommensurate contact between atomic sheets [5]. Graphene, two-dimensional crystal material, with internal layered structure

* Corresponding author.
E-mail address: zhangjunyan@licp.cas.cn (J. Zhang).

http://dx.doi.org/10.1016/j.apsusc.2017.04.057
0169-4332/

similar to graphite, exhibits excellent mechanical and tribological properties, has already become a new lubrication materials [18,19]. Recently, Sumant et al. [19] found that macroscopic superlubricity can be realized by graphene plus nanodiamonds under dry atmosphere friction. It is, however, the existing technologies cannot meet the requirements of large scale, high bear-capacity and wear-resistance of actual working conditions. At the same time, most of equipments are serving under humid air, therefore, it is necessary to realize engineering scale superlubricity with participate of water molecules from air in friction.

Taking advantage of these unique 2D structures of MoS_2 and graphene, more and more researchers have investigated the hierarchical structure for advanced application in optical, electrical and other physical properties [20–23]. In these hierarchical structures, there are many graphene/MoS_2 interfaces, which lead to the lattice mismatch between graphene and MoS_2 layers [18]. Meanwhile, theoretical calculations indicated that the frictional energy for the hierarchical structure was one order of magnitude smaller than the frictional energy in each individual constituent [24]. In addition, the hierarchical structure can prevent reaction of water molecules with MoS_2 in humid air. However, the preparation of graphene and MoS_2 hierarchical structure are mainly focused on methods like hydrothermal reaction, aqueous reduction and mechanical assembly [20–23,25]. It cannot provide adequate mechanical properties for friction application. Therefore, we develop graphitic-like amorphous carbon with short range graphene sheets and MoS_2 (GL/MoS_2) hierarchical structure thin films, by combining magnetron sputtering and pulse current plasma chemical-vapor deposition (PECVD) under heating temperature 600 °C. It has been found that the films with engineering superlubricity prepared by PECVD plus sputtering could match the requirements of large scale, high bear-capacity and wear-resistance of actual working conditions.

2. Experimental details

2.1. Films deposition

The hierarchical structure of GL/MoS_2 films were prepared by the combination method of pulse current plasma chemical-vapor deposition (PECVD) and medium frequency unbalanced magnetron sputtering on Si(100) substrates. Specifically, the GL films were prepared by method of PECVD in magnetron sputtering system using the hydrogen (40 sccm) and methane (10 sccm) under the preheated temperature of 200 °C, 400 °C and 600 °C, respectively. While the MoS_2 films sputtered by one molybdenum-disulfide target with the high purity Ar gas. Based pressure of the vacuum chamber was pumped to less than 9.9×10^{-4} Pa. Silicon wafers were sequentially ultrasonic cleaned in ethanol for 10 min before putting them into the vacuum chamber, dried in air and followed by etching with Ar^+ ions in a vacuum chamber to remove the native oxide on the substrates. Then, they were placed on the substrate holder which is 20 cm away from the sputtering targets. Prior to films deposition, silicon interlayer, about 134 nm thick, was deposited on substrates by magnetron sputtering (a target current of 0.6 A) to improve the adhesion between the substrate and films. Then multilayer films was deposited by PECVD with the pressure of 25 Pa and MoS_2 target current of 0.5 A. The multilayer films were depositied with an ABAB structure (A represents the carbon layer and B represents the MoS_2 layer) at room temperature, 200, 400 and 600 °C, respectively. The samples were obtained and defined as a-C:H/MoS_2, GL/MoS_2-200, GL/MoS_2-400 and GL/MoS_2-600. The details are shown in Table 1.

2.2. Characterizations of films

The thickness of the samples was measured by cross-section SEM images (JEOL JSM-6701F) with an energy dispersive spectroscopic (EDS) detector. The multilayer structure of the sample GL/MoS_2-600 was measured by cross-section SEM(S-4800). The detailed nano-structure of films were observed by High resolution transmission electron microscopy (HRTEM, JEOL 2010) operated at 200 kV. The samples tested by HRTEM were deposited on the NaCl substrate followed by dissolution of the NaCl substrate with water. Micro-Raman backscattering spectra of the samples were recorded on a LabRam HR800 spectrometer (HORIBA Jobin Yvon, France) operating with 532 nm (2.3 eV) Ar laser as the excitation source. Nanoindentation tests of the samples were tested (XP) using a computer controlled Hysitron Ub1 nanoindenter with depth limit 150 nm as a unity. The films were tested on the Surface Approach Sensitivity as 40%. All nanoindentation tests were achieved at room conditions of 20 °C and 30% relative humidity. A total of 3 indentations were performed for each film. A qualitative elastic recovery of the samples under study can be determined using the indentation load–unload curve. The recorded data taken from these curves for each samples calculated using the following formula:

$$R = (d_{max} - d_{res})/d_{max} \times 100\%$$

Where R (%) is the elastic recovery, d_{max} is the displacement at maximum load and

d_{res} is the residual or plastic displacement after load removal [26]. Friction tests were conducted using MFT-R4000 ball-on disc reciprocating tribometer equipped with a high precision friction force sensor (108AA Single Point Load Cell, Anyload Transducer Co., Ltd., Canada), with a force test range of 0.01 ~ 2 N and the theoretical deviations are less than 0.023% ($\leq \pm 0.00023$). All tests were performed at room temperature and relative humidity ranging from 35 to 40% the mating balls (5 mm, Al_2O_3 ball) were cleaned with acetone in an ultrasonic cleaner before each test. The reciprocating amplitude was 10 mm, the contact load was 10 N and 2 N. The average sliding speed was 200 mm/s. The corresponding wear scar morphologies of the samples were observed on a MAX 3D three-dimensional surface profiler.

3. Result and discussion

3.1. Characterization of films

As shown in Fig. 1a–d, the growth of graphitization starts with amorphous carbon and followed by preferentially continued growing on the edges of films, and finally formed in the center of films induced under the high temperature. The curved and short-range nanosheet with dimensions about 2 nm was analogous to highly disordered and randomly arranged graphitic structure (Fig. 1d), which is commonly referred to as high sp^2 bonded amorphous carbon [27]. In addition, the lattice spacing is about 0.34 nm shown in Fig. 1b agreed well with crystallographic orientation of graphite [28]. The TEM and HRTEM images (Fig. 1e and f) of MoS_2 show that the nanosheet structure was similar to GL carbon mentioned above, the lattice spacing is about 0.62 nm belongs to the distance of MoS_2 layers [29]. The film thickness decreased with the increase of temperature (Table 1), which can be ascribed to the two dimensional growth pattern and lower growth rate of the GL structure compared to pure amorphous carbon [30,31]. And the carbon layer transformed from amorphous to GL structure was also observed in Fig. 1a–d.

Fig. 2a shows the FESEM cross-section image of the GL/MoS_2 films. Uniform multilayer is observed and the thickness of MoS_2 and GL layers is about 16 and 14 nm, respectively. The silicon

Table 1
Experiment parameters.

Sample	Current(A) PECVD/Sputtering	Voltage(V) PECVD/Sputtering	Pressure(Pa) PECVD/Sputtering	Thickness(nm)
a-C:H/MoS_2	0.35/0.5	−600/−500	25/0.4	350
GL/MoS_2-200	0.35/0.5	−600/−500	25/0.4	324
GL/MoS_2-400	0.35/0.5	−600/−500	25/0.5	318
GL/MoS_2-600	0.35/0.5	−600/−500	25/0.5	310

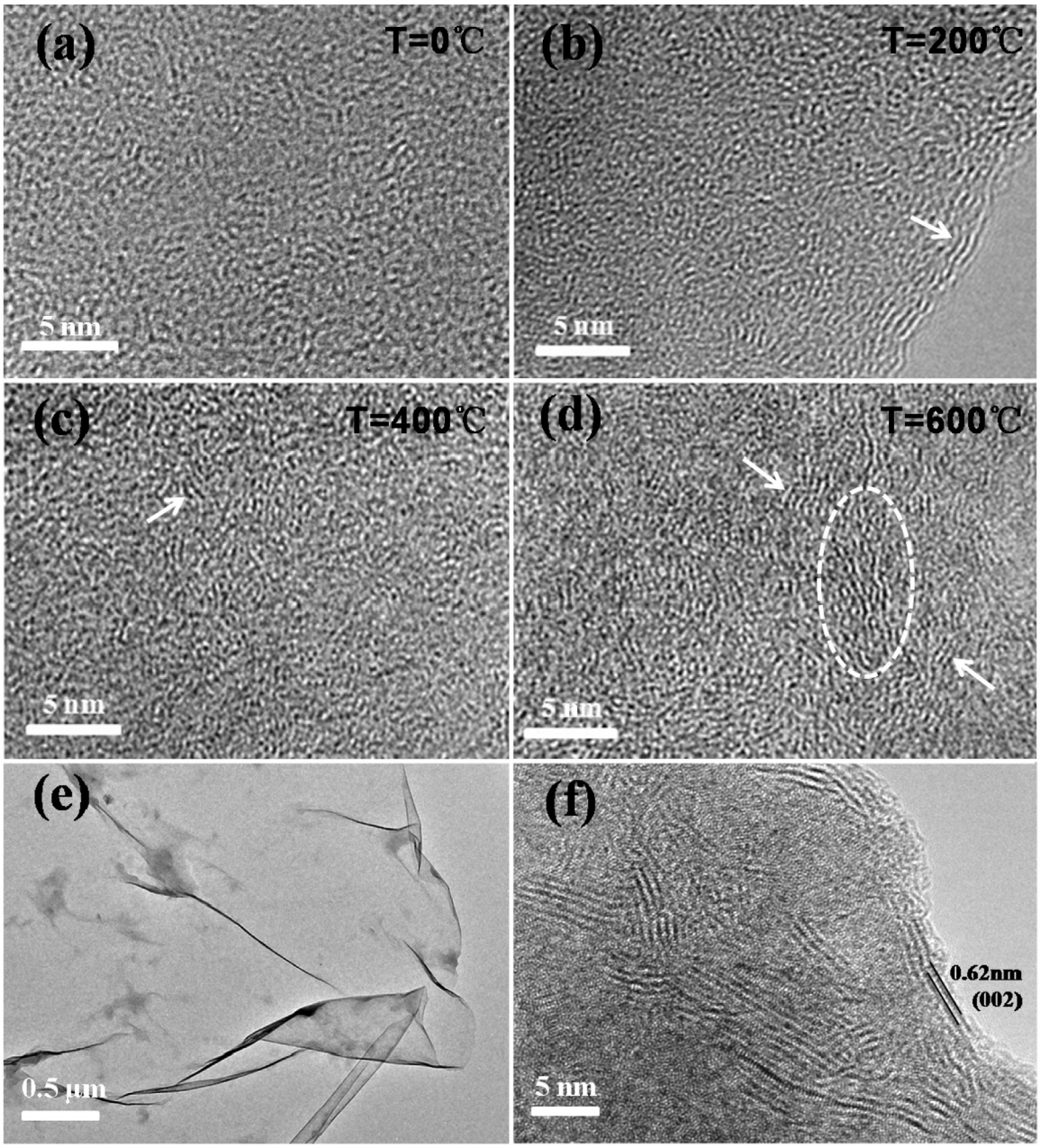

Fig. 1. (a–d) HRTEM images of a-C:H, GL/200, GL/400 and GL/600. (e,f) TEM and HRTEM images of MoS_2.

interlayer was about 81 nm, which can enhance the binding force (Fig. 2a). Raman spectroscopy is a common and effective technique to examine carbon nanomaterials such as fullerene and graphene. As depicted in Fig. 2b, the Raman spectra of samples have significant changed corresponds to the HRTEM images from amorphous carbon to GL carbon, while there's a little change for MoS_2 due to the stability of high temperature. In detail, Raman peaks at about 375 and 405 cm^{-1} correspond to the E^1_{2g} and A_{1g} mode of the hexagonal MoS_2 crystal, respectively. The E^1_{2g} mode arises from opposite vibration of two S atoms with respect to the Mo atom, whereas the A_{1g} mode is associated with the out-of-plane vibration of only S atoms in opposite direction [32,33]. To further confirm the existence of GL structure, the Raman spectra were collected in the range of 1000–4000 cm^{-1}. In Fig. 2b, the Raman spectrum exhibits the evidently separation of D, G band appearing at 1348 cm^{-1} and 1560 cm^{-1} for hybrid films, and the Raman spectra are similar

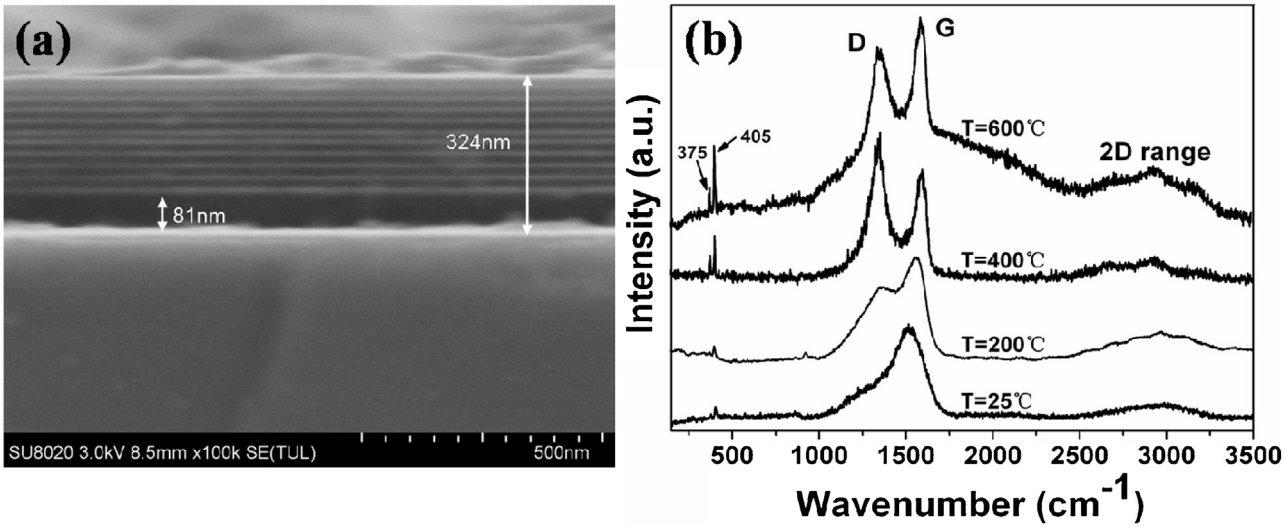

Fig. 2. (a) FESEM image of cross section of GL/MoS_2-200. (b) Raman spectum of GL/MoS_2-600, GL/MoS_2-400 GL/MoS_2-200 and a-C:H/MoS_2.

to high sp^2 graphitic carbon with high structure disorder degree [34,35]. The G band is indicative of ordered sp^2-hybridized carbon atoms in a 2D hexagonal lattice, while the D-band originates from sp^3-hybridized carbon. Moreover, the lower intensity of D band of GL/MoS_2-600 means little defects within the hybrid films compared to GL/MoS_2-400 and GL/MoS_2-200.

For further identification of MoS_2 and GL, energy dispersive X-ray spectroscopies (EDS) of HRTEM images are shown in Fig. 3. The films have a typical multilayer structure with an ABAB model. More importantly, each layer is made up of two-dimensional atom sheets, which demonstrated a multilevel lamellar structure (hierarchical structure). The EDS mapping analysis for the cross-section of GL/MoS_2-600 film reveals a layer by layer composite structure (Fig. 3a and e). The Mo and S atoms indicated multilayer structure (Fig. 3b and c). However, due to the carbon film on the micro grid, the carbon layers became blurred (Fig. 3d). Based on the comprehensive analysis of the structure, the results indicated that a kind of GL/MoS_2 film with novel hierarchical structure was prepared.

3.2. Mechanical properties

The mechanical properties of the films with hierarchical structure were investigated by the nanoindentor. Fig. 4a shows hardness and elastic modulus histogram of samples, a-C:H/MoS_2 composite structure demonstrates highest hardness (~12.5 GPa) and excellent elastic modulus (~143.7 GPa), while GL/MoS_2 films exhibit lower hardness and elastic modulus attributed to the higher sp^2 carbon with increase of temperature, inferred by HRTEM and Raman spectrum. The GL/MoS_2-600 with the lowest hardness (~7.8 GPa) and elastic modulus (~75.1 GPa) due to the very weak interlayer interaction, but that is an indirect explanation of as-desposited films with a layer by layer composite structure. Interestingly, the film shows a high elastic recovery of 86.8% and indicating that elastic or reversible deformation is predominant during indentation process.

3.3. Tribological performance

The importance of designing hierarchical structure within GL/MoS_2 to achieve superlubricity is demonstrated in this experiment. Fig. 5 presents the friction coefficient of the films as a function of sliding time under the contact load 2 N and 10 N with sliding speed of 0.2 m/s in humid air. At low contact load (2 N), as depicted in Fig. 5a, the friction coefficient of GL/MoS_2-600 achieved a very low value (<0.1) after a shorter running-in period, then the friction coefficient is quickly stable at about 0.013, close to the state of superlubricity. However, the friction coefficient of sample a-C:H/MoS_2 is about 0.079 much higher than that of GL/MoS_2 samples, obviously. At the same time, GL/MoS_2 samples show lower and lower friction coefficient with the increase of temperature from 200 °C to 600 °C. In a word, the perfect layer structure, induced by high temperature, endows the film with excellent tribological performance. In turn, the sample GL/MoS_2-600 shows super-low friction coefficient close to superlubricity owing to the hierarchical structure. To further explore the tribological performance of the sample GL/MoS_2 under higher contact load, the contact load was changed from 2 N to 10 N. When the contact load reaches 10 N, the friction coefficients were drastically reduced. Especially for GL/MoS_2-600, a super low coefficient of friction about 0.004 was achieved. Since, there are significant amounts of planar structures in the hierarchical GL/MoS_2-600 film with extremely low interlayer shear strength. [36] First-principles calculations indicated that the interlayer shear strength of fluorographene (FL)/MoS_2 heterostructure is reduced by nearly two orders of magnitude, compared with FG/FG and MoS_2/MoS_2 bilayers, reaching the superlubricity region [37].

Fig. 6a and b show the friction coefficient as a function of sliding time and cross section profile of the wear tracks inserted with 3D images of GL/MoS_2-600. It is worth noting that the steady-state superlubricity state can be maintained even after 18000 friction cycles. Furthermore, extremely low wear is presented by Fig. 6b, similar as original morphology film. Consequently, it is possible that the main wear should occur at the initial stage of the counterpart surface, and the film still has a superior wear resistance even though under a high contact pressure. The a-C:H/MoS_2 has an average friction coefficient as high as 0.048 investigated under same experiment condition. In addition, the film itself is suffered from significant wear during sliding. Therefore, the special graphite-like and MoS_2 hierarchical structure might be responsible for the significant change of nanostructure and, thus, improve the tribological properties.

4. Conclusions

In conclusion, we successfully synthesized GL/MoS_2 films with composite structure by the combination method of pulse current plasma chemical-vapor deposition (PECVD) and medium frequency

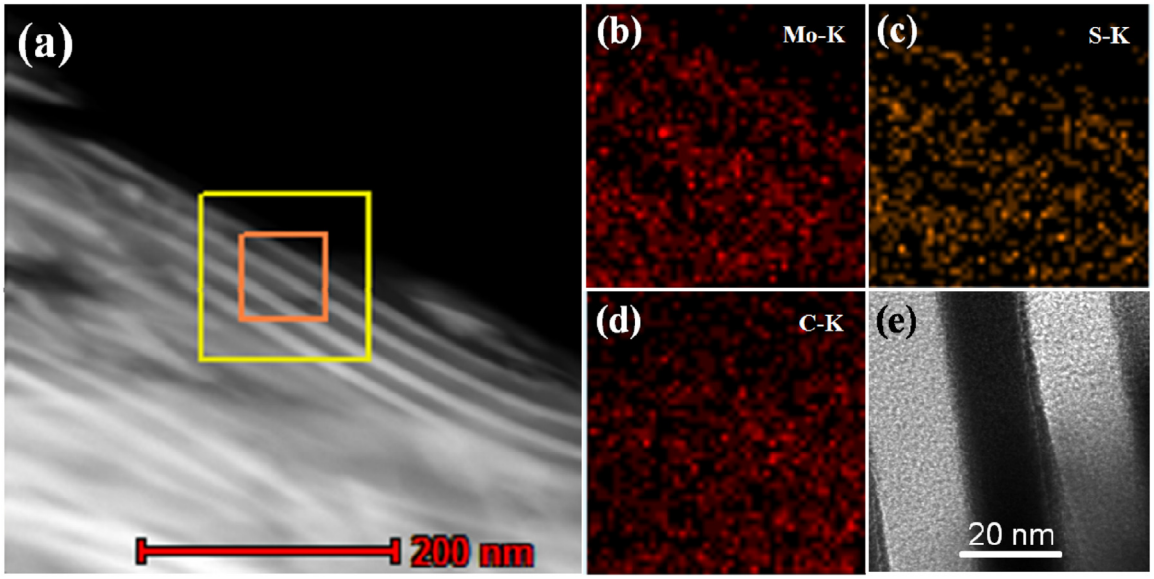

Fig. 3. (a) Dark field images of the GL/MoS_2-600 cross-section sample. (b) (c) and (d), EDS mapping of Mo, S and C atoms. (e) HRTEM image of the GL/MoS_2-600 cross-section sample.

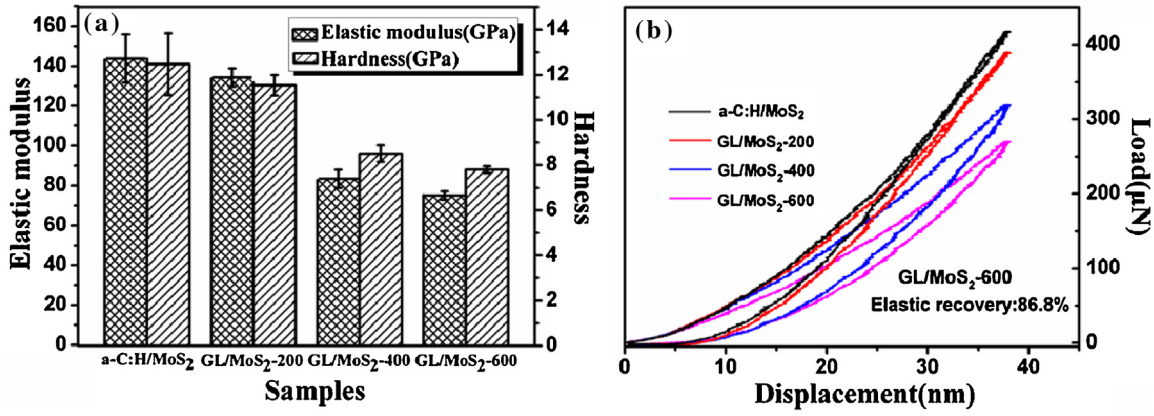

Fig. 4. (a) Hardness and elastic modulus histrogram of samples. (b) Load-displacement of a-C:H/MoS_2, GL/MoS_2-200. GL/MoS_2-400, GL/MoS_2-600.

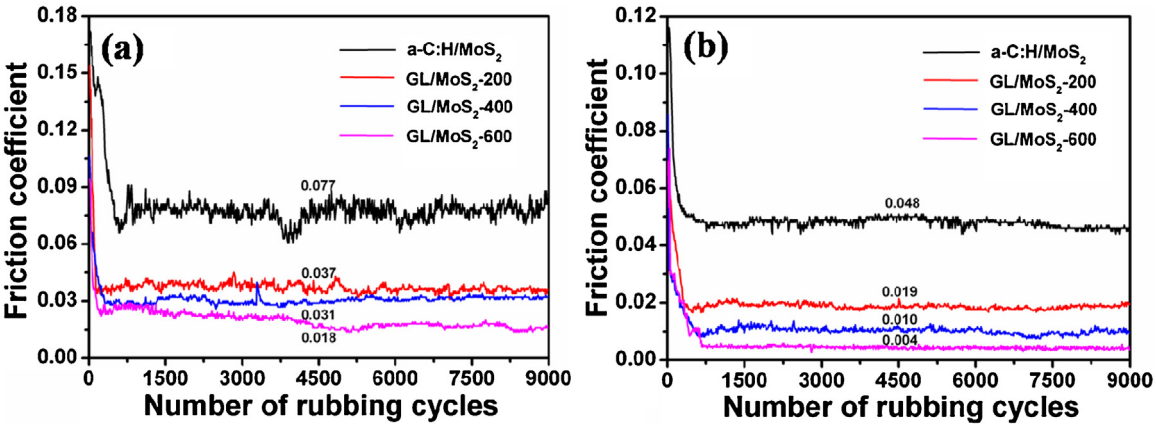

Fig. 5. (a) and (b) Friction coefficient as a function of rubbing cycles, in humid air under 2N and 10N, at a frequency of 10 Hz.

unbalanced magnetron sputtering on preheated environment. The typical graphitic-like and layered MoS_2 structures were formed in the multilayer films deposited at 600 °C. The hierarchical structure of GL/MoS_2-600 shows the super-low friction coefficient (~0.019) under low contact load and exhibits superlubricity (~0.004) under high contact load. Furthermore, the mature deposition methods and macro superlubricity properties could promote the application of GL/MoS_2 films in mechanical components.

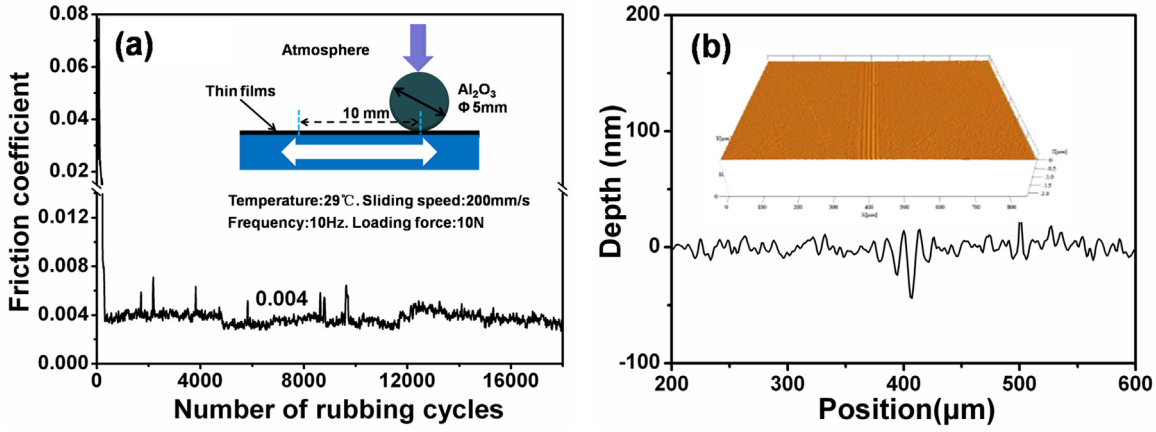

Fig. 6. (a) Friction coefficient of GL/MoS_2-600 in air under 10 N, 10 Hz. (b) The 3 D images and cross section profile of the wear tracks of GL/MoS_2-600.

Acknowledgments

The authors are grateful to the National Key Basic Research and Development (973) Program of China (Grant No. 2013CB632304) and the National Natural Science Foundation of China (Grant Nos. 51275508, 51305434), as well as the CAS "Light of West China" Program (Grant No. 51205383).

References

[1] S.S. Perry, W.T. Tysoe, Frontiers of fundamental tribological research, Tribol. Lett. 19 (2005) 151–161.
[2] M. Hirano, S. Kazumasa, Atomistic locking and friction, Phys. Rev. B 41 (1990) 11837.
[3] C. Matta, L. Joly-Pottuz, M.D.B. Bouchet, J.M. Martin, M. Kano, Q. Zhang, W.A. Goddard III, Superlubricity and tribochemistry of polyhydric alcohols, Phys. Rev. B 78 (2008) 085436.
[4] M. Chhowalla, G.A. Amaratunga, Thin films of fullerene-like MoS_2 nanoparticles with ultra-low friction and wear, Nature 407 (2000) 164–167.
[5] Z. Liu, J. Yang, F. Grey, J.Z. Liu, Y. Liu, Y. Wang, Q. Zheng, Observation of microscale superlubricity in graphite, Phys. Rev. Lett. 108 (2012) 205503.
[6] H.M. Mobarak, H.H. Masjuki, E.N. Mohamad, M.A. Kalam, H.K. Rashedul, M.M. Rashed, M. Habibullah, Tribological properties of amorphous hydrogenated (a-C:H) and hydrogen-free tetrahedral (ta-C) diamond-like carbon coatings under jatropha biodegradable lubricating oil at different temperatures, Appl. Surf. Sci. 317 (2014) 581–592.
[7] J.C. Sánchez-López, M. Belin, C. Donnet, C. Quiros, E. Elizalde, Friction mechanisms of amorphous carbon nitride films under variable environments: a triboscopic study, Surf. Coat. Technol. 160 (2002) 138–144.
[8] M. Chen, K. Kato, K. Adachi, Friction and wear of self-mated SiC and Si_3N_4 sliding in water, Wear 250 (2001) 246–255.
[9] U. Raviv, J. Klein, Fluidity of bound hydration layers, Science 297 (2002) 1540–1543.
[10] J. Klein, E. Kumacheva, D. Mahalu, D. Perahia, L.J. Fetters, Nature 370 (1994) 634–636.
[11] J. Li, C. Zhang, L. Ma, Y. Liu, J. Luo, Superlubricity achieved with mixtures of acids and glycerol, Langmuir 29 (2012) 271–275.
[12] J. Li, C. Zhang, J. Luo, Superlubricity achieved with mixtures of polyhydroxy alcohols and acids, Langmuir 29 (2013) 5239–5245.
[13] W. Tang, J. Zhang, S. Chen, N. Chen, H. Zhu, S. Ge, S. Zhang, Tactile perception of skin and skin cream, Tribol. Lett. 59 (2015) 1–13.
[14] A.P.M. Barboza, H. Chacham, C.K. Oliveira, T.F. Fernandes, E.H.M. Ferreira, B.S. Archanjo, B.R. Neves, Dynamic negative compressibility of few-layer graphene, h-BN, and MoS_2, Nano Lett. 12 (2012) 2313–2317.
[15] J.M. Martin, C. Donnet, T.L. Mogne, T. Epicier, Superlubricity of molybdenum disulphide, Phys. Rev. B 48 (1993) 10583.
[16] M. Chhowalla, G.A. Amaratunga, Thin films of fullerene-like MoS_2 nanoparticles with ultra-low friction and wear, Nature 407 (2000) 164–167.
[17] J.W. Jiang, H.S. Park, Mechanical properties of MoS_2/graphene heterostructures, Appl. Phys. Lett. 105 (2014) 033108.
[18] A.K. Geim, Graphene: status and prospects, Science 324 (2009) 1530–1534.
[19] D. Berman, S.A. Deshmukh, S.K. Sankaranarayanan, A. Erdemir, A.V. Sumant, Macroscale superlubricity enabled by graphene nanoscroll formation, Science 348 (2015) 1118–1122.
[20] M. Yang, J.M. Jeong, Y.S. Huh, B.G. Choi, High-performance supercapacitor based on three-dimensional MoS_2/graphene aerogel composites, Compos. Sci. Technol. 121 (2015) 123–128.
[21] X. Yu, R. Du, B. Li, Y. Zhang, H. Liu, J. Qu, X. An, Biomolecule-assisted self-assembly of CdS/MoS_2/graphene hollow spheres as high-efficiency photocatalysts for hydrogen evolution without noble metals, Appl. Catal. B: Environ. 182 (2016) 504–512.
[22] C. Zhai, M. Zhu, D. Bin, F. Ren, C. Wang, P. Yang, Y. Du, Two dimensional MoS_2/graphene composites as promising supports for Pt electrocatalysts towards methanol oxidation, J. Power Sources 275 (2015) 483–488.
[23] X. Zhou, Z. Wang, W. Chen, L. Ma, D. Chen, J.Y. Lee, Facile synthesis and electrochemical properties of two dimensional layered MoS_2/graphene composite for reversible lithium storage, J. Power Sources 251 (2014) 264–268.
[24] J.W. Jiang, H.S. Park, A Gaussian treatment for the friction issue of Lennard-Jones potential in layered materials: application to friction between graphene MoS_2, and black phosphorus, J. Appl. Phys. 117 (2015) 124304.
[25] S. Bertolazzi, D. Krasnozhon, A. Kis, Nonvolatile memory cells based on MoS_2/graphene heterostructures, ACS nano 7 (2013) 3246–3252.
[26] N. Hellgren, M.P. Johansson, E. Broitman, L. Hultman, J.E. Sundgren, Role of nitrogen in the formation of hard and elastic CNx thin films by reactive magnetron sputtering, Phys. Rev. B 59 (1999) 5162.
[27] M. Alfe, V. Gargiulo, R. Di Capua, F. Chiarella, J.N. Rouzaud, A. Vergara, A. Ciajolo, Wet chemical method for making graphene-like films from carbon black, ACS Appl. Mater. Interfaces 4 (2012) 4491–4498.
[28] S. Stankovich, D.A. Dikin, R.D. Piner, K.A. Kohlhaas, A. Kleinhammes, Y. Jia, R.S. Ruoff, Synthesis of graphene-based nanosheets via chemical reduction of exfoliated graphite oxide, Carbon 45 (2007) 1558–1565.
[29] L. Ze, G. Yueqiu, L. Xujun, Z. Yong, MoS_2-modified ZnO quantum dots nanocomposite: synthesis and ultrafast humidity response, Appl. Surf. Sci. 399 (2017) 330–336.
[30] X. Li, W. Cai, L. Colombo, R.S. Ruoff, Evolution of graphene growth on Ni and Cu by carbon isotope labeling, Nano Lett. 9 (2009) 4268–4272.
[31] J. Robertson, Diamond-like amorphous carbon, Mater. Sci. Eng. R: Rep. 37 (2002) 129–281.
[32] G. Plechinger, S. Heydrich, J. Eroms, D. Weiss, T. Korn, Raman spectroscopy of the interlayer shear mode in few-layer MoS_2 flakes, Appl. Phys. Lett. 1205 (2012) 1916 (arXiv preprint arXiv).
[33] H. Li, Q. Zhang, C.C.R. Yap, B.K. Tay, T.H.T. Edwin, A. Olivier, D. Baillargeat, From bulk to monolayer MoS_2: evolution of Raman scattering, Adv. Funct. Mater. 22 (2012) 1385–1390.
[34] A.C. Ferrari, Raman spectroscopy of graphene and graphite: disorder, electron–phonon coupling, doping and nonadiabatic effects, Solid State Commun. 143 (2007) 47–57.
[35] A.C. Ferrari, J. Robertson, Raman spectroscopy of amorphous, nanostructured, diamond-like carbon, and nanodiamond, Philos. Trans. R. Soc. London A: Math. Phys. Eng. Sci. 362 (2004) 2477–2512.
[36] O. Hod, The registry Index: a quantitative measure of materials' interfacial commensurability, Chem. Phys. Chem. 14 (2013) 2376–2391.
[37] L.F. Wang, T.B. Ma, Y.Z. Hu, Q. Zheng, H. Wang, J. Luo, Superlubricity of two-dimensional fluorographene/MoS_2 heterostructure: a first-principles study, Nanotechnology 25 (2014) 385701.